Electrostatic Layer-by-Layer Nanoassembly on Biological Microtemplates: Platelets

Hua Ai,[†] Ming Fang,[‡] Steven A. Jones,[†] and Yuri M. Lvov*[,‡]

Department of Biomedical Engineering and Institute for Micromanufacturing, Louisiana Tech University, Ruston, Louisiana 71272

Received December 11, 2001; Revised Manuscript Received January 29, 2002

Platelets were coated with 78-nm silica nanoparticles, 45-nm fluorescent nanospheres, or bovine immunoglobulin G (IgG) through layer-by-layer assembly by alternate adsorption with oppositely charged linear polyions. Sequential deposition on platelet surfaces of cationic poly(dimethyldiallylammonium chloride) and anionic poly(styrene sulfonate) was followed by adsorption of nanoparticles or immunoglobulins. Nano-organized shells of platelets were demonstrated by transmission electron microscopy and fluorescence microscope images. Bovine IgG was assembled on platelets, as verified with anti-bovine IgG-FITC labeling. Localized targeting of anti-IgG shelled platelets was also demonstrated. An ability to coat blood cells with nano-organized shells can have applications in cardiovascular research and targeted drug delivery.

Introduction

Platelets are blood cells with diameters in the range of 2−5 μm. They play important roles in the cardiovascular system, such as blood vessel repair, clot formation, clot retraction, clot dissolution, vasodilation, and vasoconstriction. Platelet disorders include diseases such as Bernard−Soulier syndrome, thrombasthenia, and thrombocytopenia. Physically, platelets must be able to perform basic functions, such as adhere to surfaces, aggregate with one another, and secrete their granule contents. A platelet surface is covered with at least 30 different kinds of glycoproteins[1] which affect these basic functions. Thus, the ability to alter platelet surface characteristics would allow major modifications of platelet behavior. Platelets have been modified before by methods such as cross-linking,[2] enzyme-catalyzed iodination,[3] fluorescence flow cytometry,[4] and colloidal gold labeling,[5] but the objective of these studies was to analyze platelet receptors, not to modify physical properties. Specific methods for assembly of nanostructures on platelet surfaces thus remain to be developed and exploited for medical intervention.

The technique of electrostatic layer-by-layer (LbL) assembly of oppositely charged polyions allows films to be built up on linear polyions, proteins, and nanoparticles with precise location of the components in the multilayer.[6−12] The mechanism for alternate adsorption is not restricted to electrostatic forces; biospecific interactions have also been used.[13,14] The outermost layer of a film dominates the surface charge and characterizes a specific hydrophilicity or hydrophobicity.[15] Functional proteins such as enzymes[16] and antibodies[17] remain bioactive in the LbL-assembling process. This technique has been applied to assembly of nano-organized polyion shells (containing enzymes and inorganic particles) on microtemplates, such as latex, lipid microtubules, and erythrocytes.[18−23] Hollow polyion microshells have also been fabricated as enzyme carriers.[24]

In this study, organized nanoshells have been assembled on platelets by the LbL technique. These multilayer shells contain polymers, inorganic nanoparticles, fluorescent latex and immunoglobulin G (IgG) in predetermined order with precision of a few nanometers. The present study demonstrated that is possible to target anti-IgG shelled platelets to IgG-covered regions in a silicone tubing (a model for a blood vessel).

Experimental Section

Reagents and Materials. Cationic poly(dimethyldiallylammonium chloride) (PDDA, MW 200 000, Aldrich) and anionic sodium poly(styrenesulfonate) (PSS, MW 70 000, Aldrich) were selected for the LbL assembly. To provide a physiological environment during the coating procedure, all preparation work was performed in 0.01 M PBS solution at pH 7.4. Silica nanoparticles of 78-nm diameter (Nissan Chemical Industries, Japan) and yellow-green fluorescence nanospheres (FN) of 45-nm diameter (Polysciences) were used for the assembly. PSS, silica, and FN are negatively charged, while PDDA is positively charged at pH 7.4. Solutions of 3 mg/mL PSS, 2 mg/mL PDDA, 10 mg/mL silica, and 2.5 mg/mL FN were prepared in pH 7.4 PBS.[27] The 0.5 mg/mL bovine IgG (Sigma) and 0.2 mg/mL anti-bovine IgG-FITC (Sigma) solutions were used.

Platelets Platelets were purified from fresh bovine blood. Platelet-rich plasma (PRP) was obtained through centrifugation (Eppendorf 5804R centrifuge) at 250*g* for 20 min at 22 °C. Immediate fixation of PRP in 1% paraformaldehyde solution was carried out for 2 h. Platelets were further

* To whom correspondence should be addressed. Phone: 318-257-5144. Fax: 318-257-5104. Email: ylvov@coes.latech.edu.
[†] Department of Biomedical Engineering.
[‡] Institute for Micromanufacturing.

10.1021/bm015659r CCC: $22.00
Published on Web 00/00/0000

Scheme 1. Schematic Illustration of the Electrostatic LbL Assembly on a Platelet (not to scale)[a]

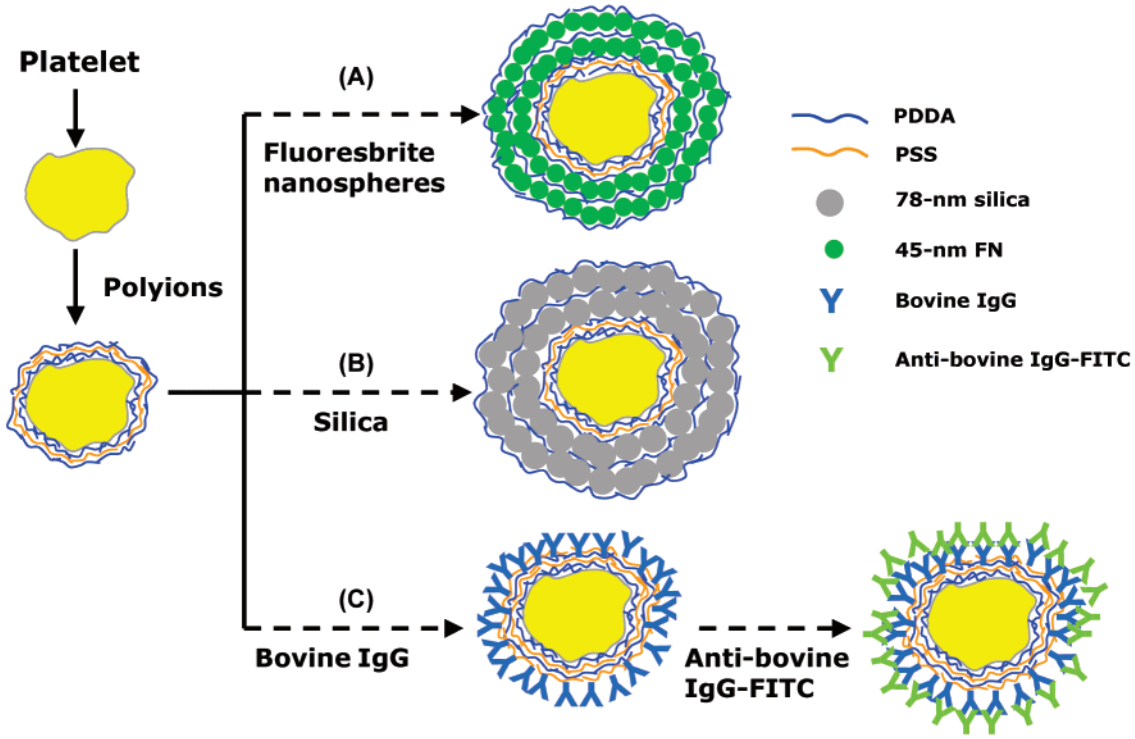

[a] Platelets were first coated with precursor layers of PDDA/PSS/PDDA. The assembly procedure followed in one of the three ways: In route A, fluorescent latex bilayers $(FN/PDDA)_2$ were added. In route B $(silica/PDDA)_2$ were assembled. In route C, immunoglobulin bilayers $(PSS/IgG)_2$ were assembled and the recognition reaction with anti-IgG-FITC was demonstrated.

purified by centrifugation at 500*g* for 5 min and dispersed in phosphate-buffered saline (PBS). The final platelet concentration was ca. 2×10^9/mL.

Instrumentation An Eppendorf 5804R centrifuge was used for the shell assembly. A quartz crystal microbalance (9-MHz QCM, USI-System Inc, Japan), transmission electron microscope (TEM, Philips-CM10, Netherlands), and fluorescent microscope (Nikon) were used for structural analysis of the nanoensembles.

Platelets Nanoassembly It is important to apply linear polycation/polyanion layers on microtemplates before assembly of proteins and nanoparticles. Flexible linear polyions cover the cell surface and act as "electrostatic glue" which holds oppositely charged nanoparticles or antibodies. A platelet surface is negatively charged because most platelet surface glycoproteins have isoelectric points lower than 7.4.[25] Scheme 1 shows three methods of an assembly to functionalize platelet shells. In route A, the outermost layers of FN/PDDA/FN were assembled by alternation of negatively charged fluorescent latex with positively charged PDDA. In route B, a silica/PDDA/silica shell was deposited. For both methods, an additional outermost layer of PDDA was assembled as a protection layer (to prevent losing silica or fluorescent nanoparticles). In method C, an immunoglobulin bilayer of composition $(PSS/IgG)_2$ was assembled.

Positively charged PDDA was first deposited on the platelets. Adsorption was allowed to proceed for 20 min to ensure complete coverage. Platelets were separated from PDDA solution by centrifugation at 550*g* for 5 min. After three washing cycles, a layer of PSS was assembled. The adsorption procedure was similar to that used for the PDDA layer. A PDDA/PSS/PDDA multilayer was assembled on platelets as a precursor before deposition of nanoparticles or IgG.

QCM Study of IgG and Anti-IgG Assembly To monitor polyion and nanoparticle layer formation on platelets at pH 7.4, the coating procedure was elaborated on 9-MHz quartz crystal microbalance (QCM, USI-System Inc, Japan) electrodes. The QCM frequency shift (ΔF) caused by the stepwise adsorption process was measured. ΔF was used to calculate mass and thickness of the layers deposited at every assembly step. For these calculations, the Sauerbrey equation was used[26] and scaling was performed.[27]

Results and Discussion

(1) Elaboration of the Polyion/Nanoparticle/Immunoglobulin Assembly on the Plane Surface. For routes A and B, the film thickness is shown for each adsorption cycle in Figure 1A. Film thickness was calculated from QCM frequency shifts.[26] A film thickness of polyions varied with ionic strength of the solutions. It was reasonable to have a 2-nm bilayer thickness for PDDA/PSS deposited at 0.137 M NaCl in PBS. Assembly steps for 78-nm silica or 45-nm FN nanoparticles were easily detected because the film thickness sharply increased. The increases in measured thickness were close to the diameters of nanoparticles used.

Assemblies of $(PSS/IgG)_5$ and $(PSS/anti\text{-}IgG)_5$ multilayers are shown in Figure 1B. Each point represents an IgG or anti-IgG adsorption layer. The prelayer sequence was PDDA/PSS/PDDA. Additional layers of $(PSS/IgG)_5$ or $(PSS/anti\text{-}IgG)_5$ were added later. The averaged frequency shift of every

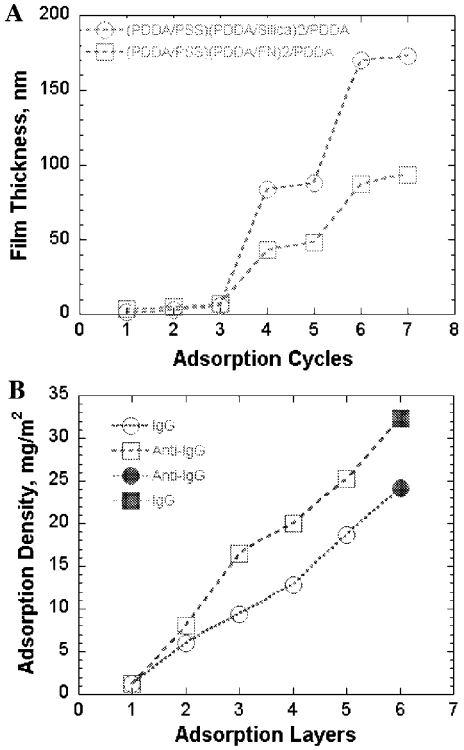

Figure 1. (A) Film thickness of each assembly layer for (PDDA/PSS)-(PDDA/silica)$_2$/PDDA and (PDDA/PSS)(PDDA/FN)$_2$/PDDA. The first three layers are 5−7 nm thick. The (PDDA/silica) layers are 78−82 nm thick, corresponding to the diameter of the silica particles. The (PDDA/FN) layers are 36−40 nm thick, corresponding again to particle diameter. (B) Adsorption density of each assembly layer for IgG and anti-IgG coatings. For (PSS/IgG)$_5$/anti-IgG, every IgG layer has an average density of 3.7 mg/m^2, the final anti-IgG layer has a density of 5.6 mg/m^2, and the final IgG layer has a density of 7.2 mg/m^2.

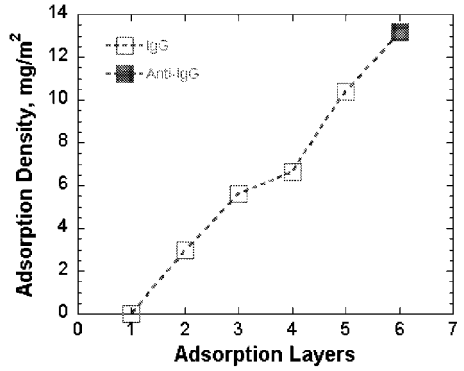

Figure 2. Assembly procedure of (PDDA/IgG)$_5$ + anti-IgG. Adsorption density of each assembly layer for IgG and anti-IgG coatings was shown in the assembly with PDDA. The averaged IgG adsorption density is 2.1 mg/m^2. The final adsorbed anti-IgG layer has a density of 2.75 mg/m^2.

IgG layer was 89 Hz. As calculated, IgG adsorption density during 30 min on QCM electrodes was 3.7 mg/m^2. To demonstrate the specific binding ability of assembled IgG, the resonator (with outermost IgG) was dipped in a solution of anti-IgG-FITC for 30 min. The bound anti-IgG-FITC layer coverage was 5.6 mg/m^2. Thus, IgG in the multilayer is specifically recognized by anti-IgG. On another electrode, multilayers of (PSS/anti-IgG)$_5$ were assembled. The outermost anti-IgG layer remained biologically active. The adsorption density of the bound IgG layer is 7.2 mg/m^2,

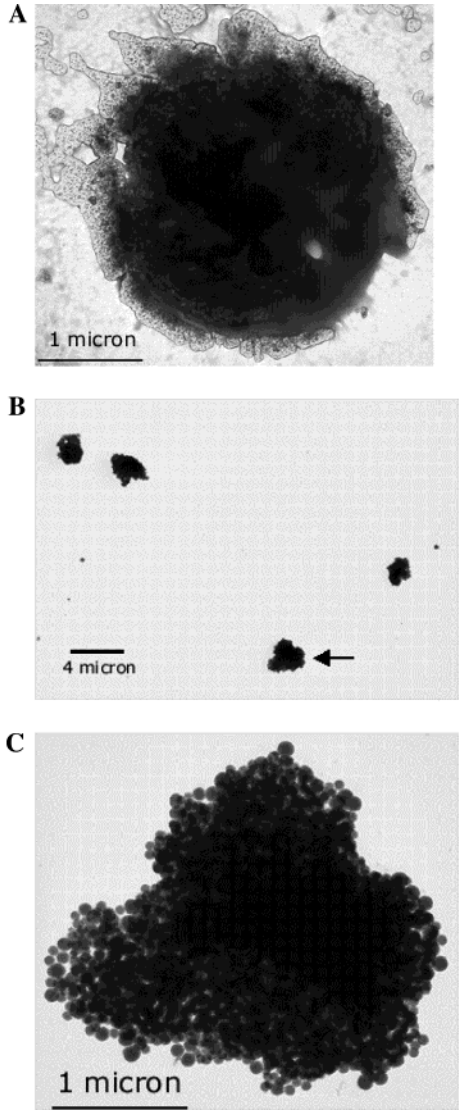

Figure 3. (A) A bovine platelet (TEM image ×21K): The platelet is intact (not a cross-sectional view). The inner components could not be clearly viewed. The platelet membrane is clearly presented. (B) Four platelets coated with 78 nm silica shell with composition PDDA/PSS/PDDA + (silica/PDDD)$_2$ (TEM ×1.65K). (C) An amplified view of a platelet (arrow) from (B) (TEM ×21K). The platelet ($D = 2.8\ \mu$m) is totally covered with 78 nm silica. The size of the platelet in (C) is close to that of the platelet in (A).

almost twice the thickness of 3.7 mg/m^2 found for the (PSS/IgG)$_5$ layers. So, more IgG was absorbed onto anti-IgG than IgG bound to PSS layer. The biological specific binding between antigens and antibodies might be stronger than electrostatic binding.

Usually the isoelectric point (PI) of IgG was near pH 7. The exact PI value of bovine IgG was not known here. The charge of IgG could be weakly negative or positive at pH 7.4. Whereas the procedure is not limited to polyanion PSS, polycation PDDA was used to assemble IgG in a separate experiment. The averaged film thickness of each IgG layer was about 2.1 mg/m^2 (Figure 2). It was much smaller than the value of 3.7 mg/m^2 for IgG adsorbed on PSS layers. The reason is not clear. Assembly of IgG was at pH 7.4, which is slightly higher than its isoelectric point.[17,28] Thus, the protein surface was approximately neutral in charge, and some additional interaction facilitated the stronger interaction

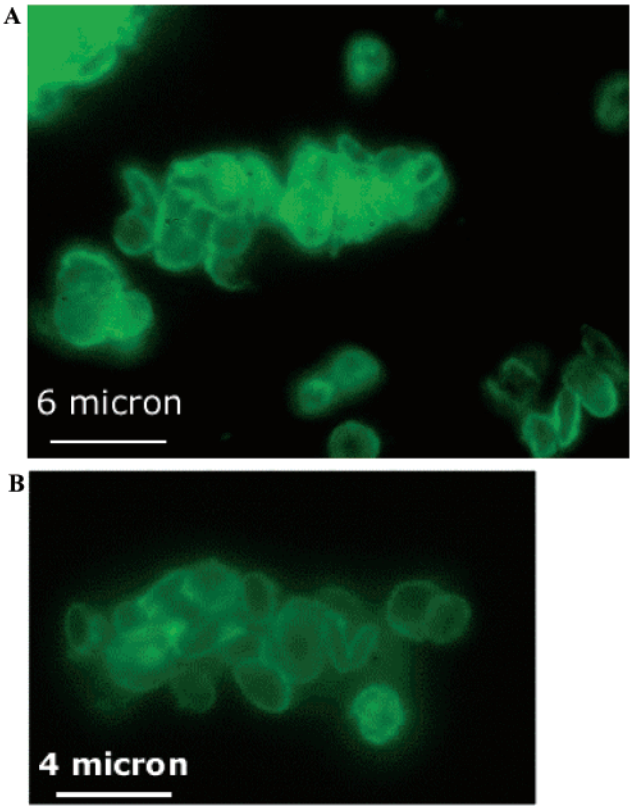

Figure 4. (A) Platelets coated with 45 nm fluorescence nanospheres (magnification: 1K). Both single platelet and clumped platelets were seen in the same field. Platelets were yellow-green in color and membranes were clearly seen. (B) Platelets assembled with bovine IgG and labeled with anti-bovine IgG-FITC (magnification: 1.8K). Platelets were clearly viewed due to fluorescent FITC.

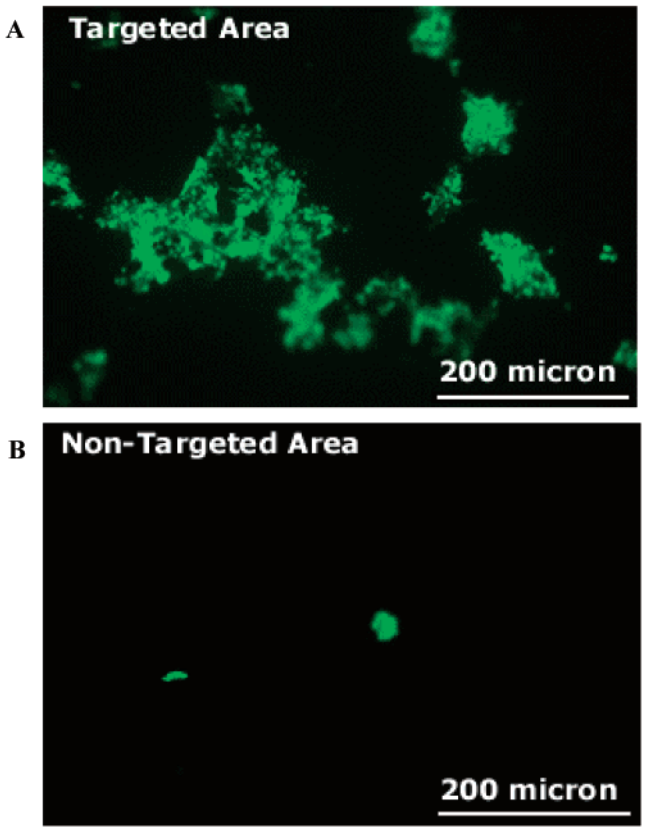

Figure 5. (A) Anti-IgG shelled platelets targeted to an area based on anti-IgG-FITC recognition of IgG-covered regions. Most of the IgG area was bound by modified platelets, and the fluorescence signal was obvious. (B) Nontargeted area. Only a few platelets are attached nonspecifically to this area.

of IgG with anionic PSS rather than with cationic PDDA. Probably, hydrophobic forces between PSS and IgG play an important role.[17] Also PSS may exhibit more roughness than PDDA, which may improve IgG adherence. The orientation of IgG molecules on the film surface is not definite. An upright position would be helpful for binding of anti-IgG.

(b) Assembly of Polyion/Nanoparticle/Antibody Coating on Platelets. Transmission electron microscopy (TEM, Philips CM10) and fluorescence microscopy (Nikon) were used to examine the results of silica nanoparticle and FN shell assembly on platelets, respectively. A bovine platelet in the initial nontreated state is shown in Figure 3A. The diameter of the platelet is 2.5 μm. In Figure 3B, four platelets coated with silica shells are presented. One of them (arrow) is presented in Figure 3C at higher magnification. The platelet (not the same one from Figure 3A) is covered with silica nanoparticles. The size of the platelet was retained after the silica encapsulation, but its shape was slightly disturbed.

In another experiment, platelets were covered with fluorescent nanospheres following the construction plan PDDA/PSS/PDDA + $(FN/PDDA)_2$, Figure 4A. These platelets have a yellow-green color under a fluorescence microscope due to FN coverage of the platelet surface, indicating full surface coverage with FN nanoparticles.

In Figure 4B we show platelets assembled with an outermost layer of $(PSS/IgG)_2$ that were exposed to a solution of fluorescent anti-IgG-FITC. Before the antigen−antibody recognition, platelets were invisible under the fluorescent microscope, but after the specific recognition reaction, the platelet membrane became visible. Thus, the IgG assembled on the platelet surface was specifically recognized and bound by anti-IgG-FITC, and immunoglobulin-covered platelets can be targeted to specific sites based on this interaction.

Next, bovine IgG was deposited through LbL self-assembly at a specific area in the silicone tubing, and the other parts of the tube remained uncovered with IgG. One-tenth of the length (8 mm) of protein-deposition-resistant silicone medical tubing was selectively coated with bovine IgG on the inner surface. A solution of platelets shelled with anti-bovine IgG-FITC was then passed through the tubing 20 times. Afterward, the tubing was rinsed, dried, and studied under a fluorescence microscope. Results are shown in Figure 5. The samples were taken from targeted (A) and nontargeted (B) areas. The fluorescence signal from the targeted areas was 154 times larger than that from nontargeted areas, indicating binding of platelets predominantly to the IgG labeled site. This experiment demonstrates the ability to target antibody-modified platelets to specific sites (expressing related antigens) in blood vessel.

Conclusion

In conclusion, nanoparticles and immunoglobulins were assembled in nano-organized shells on bovine platelets through an electrostatic LbL self-assembly technique. Plate-

lets were the second class of blood cells modified with nanoassembly after erythrocytes.[22] The coverage of 78-nm silica and 45-nm fluorescent nanospheres on platelets was studied under TEM or fluorescence microscopes. An IgG layer was adsorbed on platelets in alternation with poly(styrenesulfonate), and its specific immune recognition and targeting with fluorescent anti-IgG-FITC were demonstrated. The technique makes several platelet modifications possible. First, abnormal receptor−agonist interactions could be blocked by nanoshells. Second, platelet aggregation could be altered due to novel surface properties of the cells. Third, platelet secretion could be controlled by thickness and composition of the nanoshell. Fourth, platelets can be targeted to specific sites in a blood vessel through antibody coating. These results show that it is possible to modify biological cell properties by assembling different materials. The presented approach of organized nanoshell formation can be extended to other cells or microbes for their surface modification or encapsulation.

Acknowledgment. We thank Dr. Xiaoxi Qiao for his assistance in using TEM, Dr. James Spaulding for his help with the fluorescence microscopy, and Dr. William H. Green for providing bovine blood. This work was supported in part by NSF-0092001 Grant “Micro/Nanodevices and Systems”.

References and Notes

(1) Holmsen, H. In *Hematology*; Williams, W. J., Beutler, E., Erslev, A. J., Lichtman, M. A., Eds.; McGraw−Hill: New York, 1990; p 1189.
(2) Peters, K.; Richards, F. *Annu. Rev. Biochem.* **1977**, *46*, 523.
(3) Philips, D. *Biochemistry* **1972**, *11*, 4582.
(4) Adelman, B.; Michelson, A. D.; Handin, R. I.; Ault, K. A. *Blood* **1985**, *66*, 423.
(5) Albrecht, R. M.; Olorundare, O. E.; Simmons, S. R.; Loftus, J. C.; Mosher, D. F. *Methods in Enzymology*; Hawiger, J. J., Ed.; Academic Press: San Diego, CA, 1992; Vol. 215, pp 456−479.
(6) Decher, G.; Hong, J.-D. *Ber. Bunsen-Ges. Phys. Chem.* **1991**, *95*, 1430.
(7) Decher, G. *Science* **1997**, *227*, 1232.
(8) Lvov, Y.; Decher, G.; Möhwald, H. *Langmuir* **1993**, *9*, 481.
(9) Tsukruk, V.; Blyznyuk, V.; Visser, D.; Campbell, A.; Bunnig, T, Adams, W. *Macromolecules* **1997**, *30*, 6615.
(10) Tsukruk, V. *Prog. Polym. Sci.* **1997**, *22*, 247.
(11) Schlenoff, J. *Adv. Mater*. **1998**, *10*, 347.
(12) Mendelson, J.; Barrett, C.; Chan, V.; Pal, A.; Mayes, A.; Rubner, M. *Langmuir* **2000**, *16*, 5017.
(13) Decher, G.; Lehr, B.; Lowack, K.; Lvov, Y.; Schmitt, J. *Biosens. Bioelectron.* **1994**, *9*, 677.
(14) Anzai, J.; Kobayashi, Y.; Nakamura, N.; Nishimura, M.; Hoshi, T. *Langmuir* **1999**, *15*, 221.
(15) Yoo, D.; Shiratori, S.; Rubner, M. *Macromolecules* **1998**, *31*, 4309.
(16) Lvov, Y.; Caruso, F. *Anal. Chem.* **2001**, *73*, 4212.
(17) Caruso, F.; Niikura, K.; Furlong, D. N.; Okahata, Y. *Langmuir* **1997**, *13*, 3427.
(18) Sukhorukov, G.; Donath, E.; Davis, S.; Lichtenfeld, H.; Caruso, F.; Popov, V.; Möhwald, H. *Polym. Adv. Technol.* **1998**, *9*, 759.
(19) Donath, E.; Sukhorukov, G.; Caruso, F.; Davis, S.; Möhwald, H. *Angew. Chem, Int. Ed.* **1998**, *37*, 2202.
(20) Leporatti, S.; Voigt, A.; Mitlohner, R.; Sukhorukov, G.; Donath, E.; Mohwald, H. *Langmuir* **2000**, *16*, 4059.
(21) Caruso, F.; Caruso, R.; Möhwald, H. *Science* **1998**, *282*, 1111.
(22) Möhwald, H. *Colloids Surf.* **2000**, *171*, 25.
(23) Lvov, Y.; Munge, B.; Giraldo, O.; Ichinose, I.; Suib, S. L.; Rusling, J. F. *Langmuir* **2000**, *16*, 8850.
(24) Lvov, Y.; Antipov, A.; Mamedov, A.; Möhwald, H.; Sukhorukov, G. *Nano Lett.* **2001**, *1*, 125.
(25) McGregor, J.; Clemetson, K.; James, E.; Luscher, E.; Dechavannne, M. *Biochim. Biophys. Acta* **1980**, *599*, 473.
(26) Sauerbrey, G. *Z. Phys.* **1959**, *155*, 206.
(27) Lvov, Y.; Ariga, K.; Ichinose, I.; Kunitake, T. *J. Am. Chem. Soc.* **1995**, *117*, 6117.
(28) Buijs, J.; Lichtenbelt, J. W. Th.; Norde, W.; Lyklema, J. *Colloids Surf., B* **1995**, *5*, 11.

BM015659R